

This work has been submitted to Radiology: Artificial Intelligence for possible publication. Copyright may be transferred without notice, after which this version may no longer be accessible.

Targeted T2-FLAIR Dropout Training Improves Robustness of nnU-Net Glioblastoma Segmentation to Missing T2-FLAIR

Marco Öchsner¹, Lena Kaiser², Robert Stahl¹, Nathalie L. Albert^{2,3,4}, Thomas Liebig¹, Robert Forbrig¹, Jonas Reis¹

¹ Institute of Neuroradiology, LMU University Hospital, LMU Munich, Germany

² Department of Nuclear Medicine, LMU University Hospital, LMU Munich, Germany

³ German Cancer Consortium (DKTK), Partner site Munich, Munich, Germany

⁴ Bavarian Cancer Research Center (BZKF), Munich, Germany

Article type: Original research

Summary

Targeted T2 fluid-attenuated inversion recovery dropout preserved full-protocol glioblastoma MRI segmentation and improved Dice similarity coefficient from 66.5% to 92.6% when fluid-attenuated inversion recovery was absent.

Key points

- With all four MRI sequences available, targeted T2 fluid-attenuated inversion recovery dropout preserved segmentation performance (median overall Dice similarity coefficient, 94.8% with dropout vs 95.0% without dropout).
- With T2 fluid-attenuated inversion recovery withheld at inference, dropout training prevented performance collapse (whole-tumor Dice similarity coefficient, 60.4% vs 92.6%; edema Dice similarity coefficient, 14.0% without dropout vs 87.0% with dropout).

- With T2 fluid-attenuated inversion recovery withheld, dropout training eliminated systematic whole-tumor volume underestimation (Bland-Altman mean bias, -45.6 mL without dropout vs 0.83 mL with dropout).

Abstract

Purpose: To determine whether targeted T2 fluid-attenuated inversion recovery (T2-FLAIR) dropout training improves glioblastoma MRI tumor segmentation robustness to missing T2-FLAIR without degrading performance when T2-FLAIR is available.

Materials and Methods: This retrospective multi-dataset study developed nnU-Net models on BraTS 2021 (n=848) and externally tested them on UPenn-GBM glioblastoma MRI (n=403; 2006–2018; age 18–89 years; 60% male). Models were trained with no dropout or targeted T2-FLAIR dropout (probability rate (r)=0.35 or 0.50) by replacing only the T2-FLAIR channel with zeros. Inference used T2-FLAIR-present and T2-FLAIR-absent scenarios (T2-FLAIR set to zero). The primary endpoint was Dice similarity coefficient (DSC), secondary endpoints were 95th percentile Hausdorff distance and Bland-Altman whole-tumor volume bias. Equivalence was assessed with two one-sided tests using ± 1.5 Dice similarity coefficient percentage points, and noninferiority versus HD-GLIO used a -1.5-point margin.

Results: With T2-FLAIR present, median overall DSC was 94.8% (interquartile range, 90.0%-97.1%) with dropout and 95.0% (interquartile range, 90.3%-97.1%) without dropout (equivalence supported, $p < 0.001$). With T2-FLAIR absent, median overall DSC improved from 81.0% (interquartile range, 75.1%-86.4%) without dropout to 93.4% (interquartile range, 89.1%-96.2%) with dropout (r=0.35); edema DSC improved from 14.0% to 87.0%, edema 95th percentile Hausdorff distance improved from 22.44 mm to 2.45 mm and whole-tumor volume bias improved from -45.6 mL to 0.83 mL. Dropout was noninferior to HD-GLIO under T2-FLAIR-present (all $p < 0.001$).

Conclusion: Targeted T2-FLAIR dropout preserved segmentation performance when T2-FLAIR was available and reduced segmentation error and whole-tumor volume bias when T2-FLAIR was absent.

Introduction

Glioblastoma is the most common malignant primary brain tumor in adults and requires assessment of contrast-enhancing and non-enhancing components for treatment planning

and response assessment [1,2]. Because manual delineation of tumor compartments is time-consuming and subject to inter-reader variability, automated MRI tumor segmentation has become a key tool for quantitative volumetry and radiomics [3]. Deep learning methods, particularly U-Net-style architectures and self-configuring frameworks such as nnU-Net, have achieved strong performance and are increasingly used as standard backbones for brain tumor segmentation [4,5]. The Multimodal Brain Tumor Segmentation (BraTS) challenges have accelerated this progress by providing large, multi-institutional datasets with standardized annotations of tumor sub compartments [6,7]. However, most high-performing pipelines assume that a complete four-sequence structural MRI protocol (T1-weighted, post-contrast T1-weighted (T1-CE), T2-weighted, and T2-fluid-attenuated inversion recovery (T2-FLAIR)) is available both during training and deployment [4,8].

In routine practice and in retrospective cohorts, protocol completeness cannot be assumed. Sequences may be absent, non-diagnostic due to motion or other artefacts, or acquired with incompatible parameters, creating a common mismatch between model development conditions and deployment reality [9,10,11]. When models trained exclusively on complete four-sequence inputs are applied to studies lacking a usable sequence, segmentation quality can degrade substantially, potentially excluding patients from downstream analyses and introducing selection bias. This issue is particularly consequential for T2-FLAIR-dependent targets, including peritumoral edema and non-enhancing tumor, which contribute to comprehensive disease burden assessment [2].

Several strategies have been proposed to improve robustness to missing MRI modalities. One approach imputes missing sequences, synthesizing the absent modality using generative adversarial networks [10,12], or variational autoencoders [13], enabling inference with models that expect complete inputs. Other approaches learn modality-specific representations that can be combined from whichever inputs is available [14], or they train multiple modality-subset-specific models and select an appropriate model at inference based on available sequences [11]. An alternative is sequence (modality) dropout training, in which selected modalities are replaced with a sentinel (commonly zeros) during training, so the network learns to tolerate missing sequences without architectural changes. Prior work demonstrates that sequence dropout can preserve performance when all sequences are available while improving robustness when one or more sequences are missing [15,16,17]. However, most prior sequence-dropout studies emphasize robustness across multiple

missing-sequence combinations and provide comparatively limited external testing on independent clinical cohorts. In contrast, our study focuses on the clinically common scenario of absent or non-diagnostic T2-FLAIR and evaluates the deployment-relevant trade-off explicitly: no performance loss when T2-FLAIR is available versus robust performance when T2-FLAIR is absent. Therefore, the purpose of this multi-dataset study was to develop and externally test an nnU-Net-based glioblastoma segmentation pipeline that is robust to missing T2-FLAIR using a targeted T2-FLAIR dropout training scheme at two fixed dropout probabilities. We hypothesized that (i) targeted FLAIR dropout training would maintain segmentation quality when T2-FLAIR is present at inference, yielding Dice similarity comparable to a standard four-sequence nnU-Net, and (ii) in a prespecified T2-FLAIR-absent deployment scenario, dropout-trained models would substantially outperform standard four-sequence models for T2-FLAIR-dependent targets on both benchmark development data and an independent clinical external test cohort.

Methods

Study design and reporting

This retrospective multi-dataset study used only publicly available, de-identified imaging datasets. Accordingly, ethics approval and informed consent were not required, and the study involved no interaction with human participants. Reporting followed the Metrics Reloaded recommendations for image analysis validation, the Checklist for Artificial Intelligence in Medical Imaging (CLAIM) and its 2024 update; a completed checklist is provided in the Supplement [18,19,20].

Datasets and reference standard

We used the RSNA-ASNR-MICCAI BraTS 2021 training dataset, excluding the University of Pennsylvania glioblastoma cohort (UPenn-GBM), for model development and internal testing [7,21]. Organizer-preprocessed a four structural sequence MRI (T1, contrast-enhanced T1-CE, T2, and T2-FLAIR, 1 mm resolution, all co-registered to the T1 image and skull-stripped), and expert tumor segmentations were used (BraTS n = 848). The data are acquired at various sites and utilize different protocols and scanners.

External testing used the UPenn-GBM cohort (n = 403) comprising baseline pre-treatment MRI and expert-revised tumor segmentations [21,22,23], formally part of the BraTS training dataset but excluded in our study from all model training, to serve as an external validation

dataset. We included cases with (i) an available structural MRI including at least T1, T1-CE, and T2, and (ii) an available reference standard segmentation, T2-FLAIR was not required because one prespecified test scenario assumes T2-FLAIR is absent.

Reference standard

In both datasets, the reference standard segmentation comprises necrotic/non-enhancing tumor (NCR/NET), peritumoral edema (ED), and enhancing tumor (ET) provided by the dataset creators [7,21]. No manual edits were performed.

Output encodings and inference scenarios

We evaluated two output encodings: label-wise (NCR/NET, ED, ET; original BraTS label convention) and region-wise as used in clinical reporting (whole tumor [WT = NCR/NET \cup ED \cup ET], tumor core [TC = NCR/NET \cup ET], and ET). Two prespecified inference scenarios were evaluated: T2-FLAIR-present (T1, T1-CE, T2, T2-FLAIR) and T2-FLAIR-absent, implemented by replacing the T2-FLAIR channel with zeros after preprocessing/normalization and immediately prior to network inference. No synthetic T2-FLAIR was generated.

Model architecture and targeted T2-FLAIR dropout training

All models used the nnU-Net framework in 3D full-resolution [5]. We trained six model configurations: {label-wise, region-wise} \times {T2-FLAIR dropout probability rate (r)=0.0, 0.35, 0.50}. For the T2-FLAIR dropout models, we implemented targeted sequence dropout: the T2-FLAIR channel was replaced with zeros during training with probability p per training sample, while T1, T1-CE, and T2 were never dropped.

Training, internal testing and external testing

Models were trained on BraTS 2021 using patient-level five-fold cross-validation (80% training / 20% validation within each fold) with nnU-Net default training settings with the default number of epochs per fold ($n=1,000$). The checkpoint with the highest mean foreground DSC on the validation set was selected per fold, and at inference the cross-validation ensemble was used for each configuration. External testing applied trained configuration to all UPenn-GBM cases under both prespecified inference scenarios (T2-FLAIR-present and T2-FLAIR-absent). No UPenn-GBM data were used for training, parameter tuning, or model selection.

Comparator tool (HD-GLIO)

We benchmarked the best-performing dropout configuration against HD-GLIO, an established nnU-Net-based brain tumor segmentation tool [8], on UPenn-GBM under the T2-FLAIR-present scenario using prespecified endpoint correspondences.

Performance metrics and statistical analysis

The primary endpoint was the Dice similarity coefficient (DSC) computed per patient and per target. Secondary endpoints included the 95th percentile Hausdorff distance (HD95) and volume agreement. Volumetric agreement was assessed using Bland-Altman analysis (predicted – reference standard, mL). For inferential comparisons, equivalence of T2-FLAIR-present performance was assessed using two one-sided tests (TOST) with prespecified bounds of ± 1.5 DSC percentage points, and non-inferiority versus HD-GLIO used the same margin, as this represents a negligible difference for these types of volumetric analyses. 95% Confidence intervals were estimated by bootstrap resampling over patients (2,000 replicates). All analyses were conducted in Python (v3.12) using PyTorch 2.8, NumPy 2.3.3, SciPy 1.16.2, and pandas 2.3.3.

Results

Results are reported as median [Q1-Q3] across patients. Region-wise performance is summarized in Table 1, and label-wise performance in Supplementary Table S1.

Overall performance with T2-FLAIR available

In the T2-FLAIR-present scenario, targeted T2-FLAIR dropout training did not measurably degrade segmentation performance relative to standard four-sequence training (Table 1, Supplementary Table S1). For region-wise models, overall DSC was unchanged ($r=0$: 95.0% [90.3-97.1], $r=0.35$: 94.8% [90.0-97.1]), with comparable boundary error (HD95 $r=0$: 1.61 mm [1.14-2.72], $r=0.35$: 1.55 mm [1.14-2.74]). Class-wise performance for WT, TC, and ET was similarly stable across dropout settings (Table 1), and the label-wise models showed the same pattern across NCR/NET, ED, and ET (Supplementary Table S1). Equivalence testing supported equivalence of $r=0.35$ versus $r=0.0$ within ± 1.5 DSC percentage points across endpoints in the T2-FLAIR-present setting (TOST $p < 0.001$ throughout, see Table 2 and Supplementary Table S2).

Performance without T2-FLAIR

In the T2-FLAIR-absent scenario, standard four-sequence models trained without dropout showed a pronounced performance collapse in targets that depend strongly on T2-FLAIR

signal, whereas dropout-trained models maintained high performance (see Table 1 and Supplementary Table S1). For region-wise models, overall DSC decreased to 81.0% [75.1-86.4] without dropout but remained high with dropout ($r=0.35$: 93.4% [89.1-96.2], $r=0.5$: 93.7% [89.1-96.2]). The largest improvements were observed for WT: WT DSC increased from 60.4% [45.7-71.9] ($r=0.0$) to 92.6% [88.7-95.2] ($r=0.35$) (Table 1, Figures 1-2).

The label-wise models demonstrated the same failure mode centered on edema (Supplementary Table S1). Without dropout, edema DSC dropped to 14.0% [3.0-28.0] with large boundary error (HD95 22.44 mm [16.43-31.03]). With dropout, edema performance recovered to 87.0% [78.0-92.0] (HD95 2.45 mm [1.73-4.69]) at $r=0.35$ and 88.0% [79.0-92.0] (HD95 2.24 mm [1.73-4.64]) at $r=0.5$ (Supplementary Table S1). Consistent with these large shifts, equivalence was not supported for $r=0.35$ versus $r=0.0$ in the T2-FLAIR-absent setting (TOST $p \approx 1$ across endpoints, Table 2 and Supplementary Table S2), reflecting differences far exceeding the ± 1.5 percentage-point equivalence margin.

Sensitivity to dropout probability rate

Differences between $r=0.35$ and $r=0.50$ dropout were small in both inference scenarios. Median paired differences were minimal, and equivalence within ± 1.5 DSC percentage points was supported across endpoints (TOST $p < 0.001$, Table 3 and Supplementary Table S3). Taken together, $r=0.35$ provided robust T2-FLAIR-absent performance while preserving T2-FLAIR-present accuracy.

Volume bias and agreement

Bland-Altman analysis of whole-tumor volume in the T2-FLAIR-absent scenario demonstrated pronounced systematic under-segmentation for the no-dropout region model, with mean volume bias (predicted - reference standard) of -45.6 mL (95% bootstrap CI -48.8 to -42.6 mL) and wide limits of agreement (-108.0 to 16.8 mL). In contrast, dropout training largely eliminated this bias: the $r=0.35$ model showed a mean bias of 0.83 mL (95% CI -0.28 to 1.92 mL) with tighter limits of agreement (-20.8 to 22.5 mL). A similar pattern was observed for $r=0.5$ (bias 0.36 mL, limits of agreement -21.2 to 22.0 mL). Bland-Altman plots for $r=0.0$ and $r=0.35$ are shown in Figure 3.

Comparison to an established tool (HD-GLIO)

Under the T2-FLAIR-present scenario, we benchmarked the $r=0.35$ dropout models against HD-GLIO using the prespecified endpoint correspondences (ET vs CE, edema vs NE, and WT vs NE+CE). Across all endpoints, the $r=0.35$ models were non-inferior (all $p < 0.001$, Table 4) and

achieved higher median DSC: edema 91.77% [84.91-95.55] versus 87.68% [78.30-92.30], enhancing tumor 93.96% [87.49-96.80] versus 90.31% [83.79-93.40], and whole tumor 95.65% [91.94-97.81] versus 91.01% [84.77-94.24] (Table 4).

Discussion

In this multi-dataset study we evaluated a pragmatic application question: can targeted T2-FLAIR dropout training improve robustness to missing or non-diagnostic T2-FLAIR without degrading performance when T2-FLAIR is available? Across both label- and region-wise nnU-Net models, the results support an affirmative answer. When all four sequences were provided, dropout-trained models achieved segmentation performance that was statistically equivalent to standard four-sequence training within prespecified equivalence bounds, indicating no measurable penalty in the complete protocol setting. In contrast, when T2-FLAIR was withheld at inference to emulate an incomplete-protocol scenario, conventional four-sequence models showed a marked performance collapse for T2-FLAIR-dependent targets, most prominently edema and whole tumor, while T2-FLAIR dropout models largely preserved accuracy. Improvements were reflected in boundary error and were clinically meaningful in volumetric terms, shifting whole-tumor volume bias from substantial underestimation toward near-zero. Together, these findings provide evidence that a simple, targeted training intervention can prevent catastrophic failures when a key sequence is absent while maintaining performance when it is present [5,7,21].

Prior work has proposed several strategies for handling missing MRI modalities including modality completion (e.g., generative synthesis of missing sequences) [10,12], joint completion-segmentation approaches [24,25] and hetero-modal representation learning [14]. Sequence/modality dropout is a complementary strategy in which the segmentation network is trained to tolerate absent inputs without architectural changes. Feng and colleagues demonstrated that sequence dropout can preserve performance when all sequences are available and improve robustness when sequences are missing in BraTS-style tumor segmentation [17]. Our work is complementary but distinct in its deployment orientation: we (i) target the clinically common failure mode of missing or absent or non-diagnostic T2-FLAIR rather than modeling arbitrary missingness patterns, (ii) externally validate our models on the UPenn-GBM data with expert reference standard segmentations, and (iii) quantify deployment consequences using equivalence testing (to establish preserved performance

when T2-FLAIR is present) and Bland-Altman volumetry (to measure systematic bias when T2-FLAIR is absent).

The observed error pattern in the T2-FLAIR-absent setting is mechanistically plausible and clinically interpretable. Edema and non-enhancing tumor components are typically characterized by T2/T2-FLAIR hyperintensity, a model trained exclusively on complete four-sequence inputs can implicitly learn a reliance on T2-FLAIR for these targets and fail to exploit complementary cues from T2-weighted imaging alone. Targeted T2-FLAIR dropout repeatedly exposes the network to a mixture of complete and T2-FLAIR-absent inputs during training, encouraging reliance on redundant information in the remaining contrasts and reducing sensitivity to a single missing channel. The relative stability of enhancing tumor segmentation across conditions is expected because it is driven primarily by the T1-CE signal [2,7].

Practically, this matters for both retrospective multi-center research and clinical pipelines: missing or unusable T2-FLAIR can reduce cohort size and introduce selection bias, and systematic under-segmentation of whole tumor can compromise volumetry and derived biomarkers. The marked improvement in Bland-Altman whole-tumor volume bias in the no-T2-FLAIR setting suggests that the benefit extends beyond voxel overlap and supports more reliable quantitative volumetry, which is a central requirement for downstream response assessment and radiomics. Performance was similar for 35% and 50% T2-FLAIR dropout, suggesting that a single default dropout (e.g., $r=0.35$) may be sufficient for many pipelines and that robustness is driven primarily by exposure to missing T2-FLAIR inputs rather than by fine calibration of the dropout probability rate. Benchmarking against an established tool (HD-GLIO) further suggests that the proposed approach is competitive under the T2-FLAIR-present condition, although such comparisons are inherently sensitive to differences in preprocessing, training data, and label conventions [8]. For these reasons, benchmarking is most informative as a practical performance reference rather than a definitive head-to-head determination.

This study has several limitations. First, although UPenn-GBM provides a large independent external test cohort, it represents a single center; multi-site external testing would further strengthen evidence of generalizability across scanners, vendors, and acquisition protocols. Second, the “missing T2-FLAIR” condition was implemented in a controlled and reproducible manner by replacing the T2-FLAIR channel with zeros at inference for all participants. This

design does not fully capture failure modes such as motion-degraded T2-FLAIR, partial coverage, intensity non-standardization, or mis-registration, and as such requires identification of low-quality acquisitions. Third, we evaluated a targeted missingness pattern (T2-FLAIR), and robustness to other missing sequences (e.g., T1-CE) or combinations of missing/low-quality inputs may require different strategies and remains to be studied. Consequently, future work should evaluate the approach under more realistic missingness and degradation patterns, and across additional external cohorts with genuinely missing or non-diagnostic T2-FLAIR. Given that abbreviated MRI protocols are sometimes used in time-constrained or motion-prone settings, future studies should also assess whether segmentation performance and volumetric agreement remain acceptable when T2-FLAIR is omitted for segmentation-driven endpoints (e.g., volumetry), while separately confirming diagnostic adequacy for routine clinical interpretation. Direct comparison against a dedicated three-sequence model trained without T2-FLAIR would also help quantify the practical benefit of a single robust model versus modality-specific deployment strategies.

In conclusion, targeted T2-FLAIR dropout training within an nnU-Net segmentation pipeline provided a practical and effective strategy for robust glioblastoma MRI segmentation in a common deployment scenario of missing or unusable T2-FLAIR. This approach maintained performance when T2-FLAIR was available and substantially mitigated performance collapse, boundary error, and volumetric bias when T2-FLAIR was absent, without architectural changes or additional synthesis components. These results support targeted sequence dropout as a low-friction default strategy for multi-center glioblastoma segmentation workflows and for retrospective cohorts where protocol completeness cannot be assumed.

Acknowledgements

Generative artificial intelligence (AI) was used for manuscript preparation only. ChatGPT (OpenAI; GPT-5.2) was used to improve clarity and scientific tone. The authors performed all study conceptualization, analyses, interpretation, and critical reasoning, and take full responsibility for the final manuscript. No patient-identifiable or confidential information was entered into the AI tool.

Data and Code sharing statement

Data availability: No new imaging data were generated for this study. The MRI data and reference standard segmentations used for model development and external testing are available from public repositories under their respective data use agreements (e.g., BraTS 2021 and UPenn-GBM). The authors did not redistribute these datasets.

Code availability: All code used for preprocessing, training, inference, and statistical analysis is stored in a GitHub repository and will be made available to readers as described below:
GitHub repository: <https://github.com/LMU-NRAD/FLAIR-dopout>

Release status: private during peer review, to be made public upon acceptance

License: Apache-2.0

References

1. Weller, M., et al., *EANO guidelines on the diagnosis and treatment of diffuse gliomas of adulthood*. Nat Rev Clin Oncol, 2021. **18**(3): p. 170-186. doi: 10.1038/s41571-020-00447-z.
2. Wen, P.Y., et al., *RANO 2.0: Update to the Response Assessment in Neuro-Oncology Criteria for High- and Low-Grade Gliomas in Adults*. J Clin Oncol, 2023. **41**(33): p. 5187-5199. doi: 10.1200/JCO.23.01059.
3. Kruser, T.J., et al., *NRG brain tumor specialists consensus guidelines for glioblastoma contouring*. J Neurooncol, 2019. **143**(1): p. 157-166. doi: 10.1007/s11060-019-03152-9.
4. Dorfner, F.J., et al., *A review of deep learning for brain tumor analysis in MRI*. NPJ Precis Oncol, 2025. **9**(1): p. 2. doi: 10.1038/s41698-024-00789-2.
5. Isensee, F., et al., *nnU-Net: a self-configuring method for deep learning-based biomedical image segmentation*. Nat Methods, 2021. **18**(2): p. 203-211. doi: 10.1038/s41592-020-01008-z.
6. Menze, B.H., et al., *The Multimodal Brain Tumor Image Segmentation Benchmark (BRATS)*. IEEE Trans Med Imaging, 2015. **34**(10): p. 1993-2024. doi: 10.1109/TMI.2014.2377694.
7. Baid, U., et al., *The RSNA-ASNR-MICCAI BraTS 2021 Benchmark on Brain Tumor Segmentation and Radiogenomic Classification*. arXiv 2021. doi: 10.48550/arXiv.2107.02314.
8. Kickingreder, P., et al., *Automated quantitative tumour response assessment of MRI in neuro-oncology with artificial neural networks: a multicentre, retrospective study*. Lancet Oncol, 2019. **20**(5): p. 728-740. doi: 10.1016/S1470-2045(19)30098-1.
9. Tajbakhsh, N., et al., *Embracing imperfect datasets: A review of deep learning solutions for medical image segmentation*. Med Image Anal, 2020. **63**: p. 101693. doi: 10.1016/j.media.2020.101693.

10. Moshe, Y.H., et al., *Handling Missing MRI Data in Brain Tumors Classification Tasks: Usage of Synthetic Images vs. Duplicate Images and Empty Images*. *J Magn Reson Imaging*, 2024. **60**(2): p. 561-573. doi: 10.1002/jmri.29072.
11. Ruffle, J.K., et al., *Brain tumour segmentation with incomplete imaging data*. *Brain Commun*, 2023. **5**(2): p. fcad118. doi: 10.1093/braincomms/fcad118.
12. Conte, G.M., et al., *Generative Adversarial Networks to Synthesize Missing T1 and FLAIR MRI Sequences for Use in a Multisequence Brain Tumor Segmentation Model*. *Radiology*, 2021. **299**(2): p. 313-323. doi: 10.1148/radiol.2021203786.
13. Hamghalam, M., et al. *Modality Completion via Gaussian Process Prior Variational Autoencoders for Multi-modal Glioma Segmentation*. in *Medical Image Computing and Computer Assisted Intervention – MICCAI 2021*. 2021. Cham: Springer International Publishing. doi: 10.1007/978-3-030-87234-2_42.
14. Havaei, M., et al. *HeMIS: Hetero-Modal Image Segmentation*. in *Medical Image Computing and Computer-Assisted Intervention – MICCAI 2016*. 2016. Cham: Springer International Publishing. doi: 10.1007/978-3-319-46723-8_54.
15. Xing, J. and J. Zhang, *Segmentation of Brain Tumors Using a Multi-Modal Segment Anything Model (MSAM) with Missing Modality Adaptation*. *Bioengineering (Basel)*, 2025. **12**(8). doi: 10.3390/bioengineering12080871.
16. Novosad, P., R.A.D. Carano, and A.P. Krishnan. *A Task-Conditional Mixture-of-Experts Model for Missing Modality Segmentation*. in *Medical Image Computing and Computer Assisted Intervention – MICCAI 2024*. 2024. Cham: Springer Nature Switzerland. doi: 10.1007/978-3-031-72114-4.
17. Feng, X., et al., *Brain Tumor Segmentation for Multi-Modal MRI with Missing Information*. *J Digit Imaging*, 2023. **36**(5): p. 2075-2087. doi: 10.1007/s10278-023-00860-7.
18. Maier-Hein, L., et al., *Metrics reloaded: recommendations for image analysis validation*. *Nat Methods*, 2024. **21**(2): p. 195-212. doi: 10.1038/s41592-023-02151-z.
19. Tejani, A.S., et al., *Checklist for Artificial Intelligence in Medical Imaging (CLAIM): 2024 Update*. *Radiol Artif Intell*, 2024. **6**(4): p. e240300. doi: 10.1148/ryai.240300.
20. Mongan, J., L. Moy, and C.E. Kahn, Jr., *Checklist for Artificial Intelligence in Medical Imaging (CLAIM): A Guide for Authors and Reviewers*. *Radiol Artif Intell*, 2020. **2**(2): p. e200029. doi: 10.1148/ryai.2020200029.
21. Bakas, S., et al., *The University of Pennsylvania glioblastoma (UPenn-GBM) cohort: advanced MRI, clinical, genomics, & radiomics*. *Sci Data*, 2022. **9**(1): p. 453. doi: 10.1038/s41597-022-01560-7.

22. Clark, K., et al., *The Cancer Imaging Archive (TCIA): maintaining and operating a public information repository*. *J Digit Imaging*, 2013. **26**(6): p. 1045-57. doi: 10.1007/s10278-013-9622-7.
23. Bakas, S., et al., *Multi-parametric magnetic resonance imaging (mpMRI) scans for de novo Glioblastoma (GBM) patients from the University of Pennsylvania Health System (UPENN-GBM) (Version 2) [Data set]*. The Cancer Imaging Archive., 2021. doi: 10.1038/s41597-022-01560-7.
24. Zhou, T., et al., *Latent Correlation Representation Learning for Brain Tumor Segmentation With Missing MRI Modalities*. *IEEE Transactions on Image Processing*, 2021. **30**: p. 4263-4274. doi: 10.1109/TIP.2021.3070752.
25. Dorent, R., et al. *Hetero-Modal Variational Encoder-Decoder for Joint Modality Completion and Segmentation*. in *Medical Image Computing and Computer Assisted Intervention – MICCAI 2019*. 2019. Cham: Springer International Publishing. doi: 10.1007/978-3-030-32245-8.

Tables

Table 1: External testing on UPenn-GBM (n=403): segmentation performance of region-wise models with and without T2-FLAIR at inference. Performance of region-wise nnU-Net models (WT, TC, ET) trained on BraTS 2021 with targeted T2-FLAIR dropout probability $p = 0.0, 0.35, 0.50$ and evaluated under two prespecified inference scenarios: T2-FLAIR-present (all four sequences provided) and FLAIR-absent (T2-FLAIR channel replaced with zeros). Values are median [Q1-Q3] across patients. Overall denotes the unweighted macro-average across WT, TC, and ET.

Metrics/abbreviations: DSC = Dice similarity coefficient (reported as %); HD95 = 95th-percentile Hausdorff distance (mm); WT = whole tumor; TC = tumor core; ET = enhancing tumor; FLAIR = fluid-attenuated inversion recovery; r = dropout probability rate.

	Overall		Whole Tumor		Enhancing Tumor		Tumor Core	
T2-FLAIR drop for training	DSC med [Q1-Q3]	HD95 med [Q1-Q3]	DSC med [Q1-Q3]	HD95 med [Q1-Q3]	DSC med [Q1-Q3]	95HD med [Q1-Q3]	DSC med [Q1-Q3]	HD95 med [Q1-Q3]
<i>Segmentation with FLAIR input</i>								
r=0.0	95.0 [90.3-97.1]	1.61 [1.14-2.72]	95.5 [91.9-97.8]	1.73 [1.00-3.32]	94.1 [87.6-96.8]	1.00 [1.00-1.41]	96.5 [92.9-98.1]	1.41 [1.00-2.45]
r=0.35	94.8 [90.0-97.1]	1.55 [1.14-2.74]	95.6 [91.9-97.8]	1.62 [1.00-3.32]	94.0 [87.5-96.8]	1.00 [1.00-1.41]	96.4 [92.9-98.0]	1.41 [1.00-2.45]
r=0.5	94.8 [90.2-97.0]	1.61 [1.14-2.71]	95.3 [91.9-97.7]	1.73 [1.00-3.46]	93.7 [87.4-96.7]	1.00 [1.00-1.41]	96.5 [92.8-98.1]	1.41 [1.00-2.45]
<i>Segmentation without FLAIR input</i>								
r=0.0	81.0 [75.1-86.4]	7.59 [5.31-11.21]	60.4 [45.7-71.9]	17.24 [11.66-24.20]	92.4 [86.3-95.6]	1.00 [1.00-1.73]	94.4 [89.8-96.7]	2.45 [1.73-4.58]
r=0.35	93.4 [89.1-96.2]	2.02 [1.41-3.41]	92.6 [88.7-95.2]	2.45 [1.73-5.00]	93.5 [87.5-96.4]	1.00 [1.00-1.41]	96.2 [92.4-97.8]	1.73 [1.00-2.83]
r=0.5	93.7 [89.1-96.2]	2.03 [1.41-3.46]	93.0 [89.4-95.7]	2.24 [1.41-4.64]	93.7 [87.4-96.5]	1.00 [1.00-1.41]	96.2 [92.5-97.8]	1.73 [1.00-2.83]

Table 2: External testing on UPenn-GBM (n=403): equivalence testing (TOST) for $r=0.35$ vs $r=0.0$ across inference scenarios (region-wise). Paired comparison of region-wise models trained with targeted T2-FLAIR dropout ($r=0.35$) versus no dropout ($r=0.0$) under T2-FLAIR-present and T2-FLAIR-absent inference scenarios. Entries report the median paired DSC difference ($r=0.35 - r=0.0$) in DSC percentage points, with 95% bootstrap confidence intervals. TOST p-values test equivalence within prespecified bounds of ± 1.5 DSC percentage points ($\alpha=0.05$).

Abbreviations: TOST = two one-sided tests; DSC = Dice similarity coefficient; WT = whole tumor; TC = tumor core; ET = enhancing tumor; FLAIR = fluid-attenuated inversion recovery; r = dropout probability rate.

	Median DSC $r(0.35)-r(0.0)$ [95%CI]	TOST p-Value
<i>Segmentation with T2-FLAIR input</i>		
Overall	-0.017 [-0.046, 0.014]	<0.001
ET	-0.04 [-0.094, -0.006]	<0.001
TC	-0.011 [-0.040, 0.015]	<0.001
WT	-0.005 [-0.029, 0.023]	<0.001
<i>Segmentation without T2-FLAIR input</i>		
Overall	11.35 [10.63, 12.21]	1
ET	0.75 [0.663, 0.837]	0.98
TC	1.12 [0.97, 1.29]	1
WT	31.1 [28.2, 33.48]	1

Table 3: External testing on UPenn-GBM (n=403): equivalence testing (TOST) for $r=0.35$ vs $r=0.50$ across inference scenarios (region-wise). Paired comparison of region-wise models trained with targeted T2-FLAIR dropout probabilities $r=0.35$ versus $r=0.50$, evaluated under T2-FLAIR-present and FLAIR-absent inference scenarios. Entries report the median paired DSC difference ($r=0.35 - r=0.50$) in DSC percentage points, with 95% bootstrap confidence intervals. TOST p-values test equivalence within ± 1.5 DSC percentage points ($\alpha=0.05$).

Abbreviations: TOST = two one-sided tests; DSC = Dice similarity coefficient; WT = whole tumor; TC = tumor core; ET = enhancing tumor; FLAIR = fluid-attenuated inversion recovery; r = dropout probability rate.

	Median DSC $r(0.35)-r(0.50)$ [95%CI]	TOST p-Value
<i>Segmentation with T2-FLAIR input</i>		
Overall	0.075 [0.049, 0.093]	<0.001
ET	0.034 [0.003, 0.066]	<0.001
TC	0.049 [0.028, 0.067]	<0.001
WT	0.075 [0.038, 0.108]	<0.001
<i>Segmentation without T2-FLAIR input</i>		
Overall	-0.113 [-0.146, -0.076]	<0.001
ET	-0.061 [-0.10, -0.006]	<0.001
TC	-0.035 [-0.054, -0.018]	<0.001
WT	-0.201 [-0.233, -0.140]	<0.001

Table 4: External testing on UPenn-GBM (n=403): non-inferiority of r=0.35 dropout models versus HD-GLIO (FLAIR-present scenario). Comparison of targeted T2-FLAIR dropout models (r=0.35) with HD-GLIO under the T2-FLAIR-present inference scenario. Endpoints were compared using the following prespecified correspondences: ET (BraTS) vs CE (HD-GLIO); ED (BraTS label-wise edema) vs NE (HD-GLIO); and WT (BraTS region-wise) vs NE+CE (HD-GLIO). Values are median DSC (%) [Q1-Q3]. “Median Δ DSC” denotes the paired median difference (model – HD-GLIO) in DSC percentage points. Non-inferiority p-values correspond to a one-sided test with a prespecified non-inferiority margin of –1.5 DSC percentage points ($\alpha=0.05$).

Abbreviations: DSC = Dice similarity coefficient; ET = enhancing tumor; ED = edema; WT = whole tumor; CE = contrast enhancing; NE = non-enhancing; r = dropout probability rate.

BraTS Label/Region	HD-Glio Label	r=0.35 Median DSC (%) [Q1-Q3]	HD-GLIO Median DSC (%) [Q1-Q3]	Median Δ DSC (%) (model - HD)	Non-inferior p-Value
Edema	NE	91.77 [84.91-95.55]	87.68 [78.30-92.30]	3.158 [2.733, 3.792]	<0.001
ET	CE	93.96 [87.49-96.80]	90.31 [83.79-93.40]	3.026 [2.698, 3.262]	<0.001
WT	NE+CE	95.65 [91.94-97.81]	91.01 [84.77-94.24]	4.087 [3.702, 4.360]	<0.001

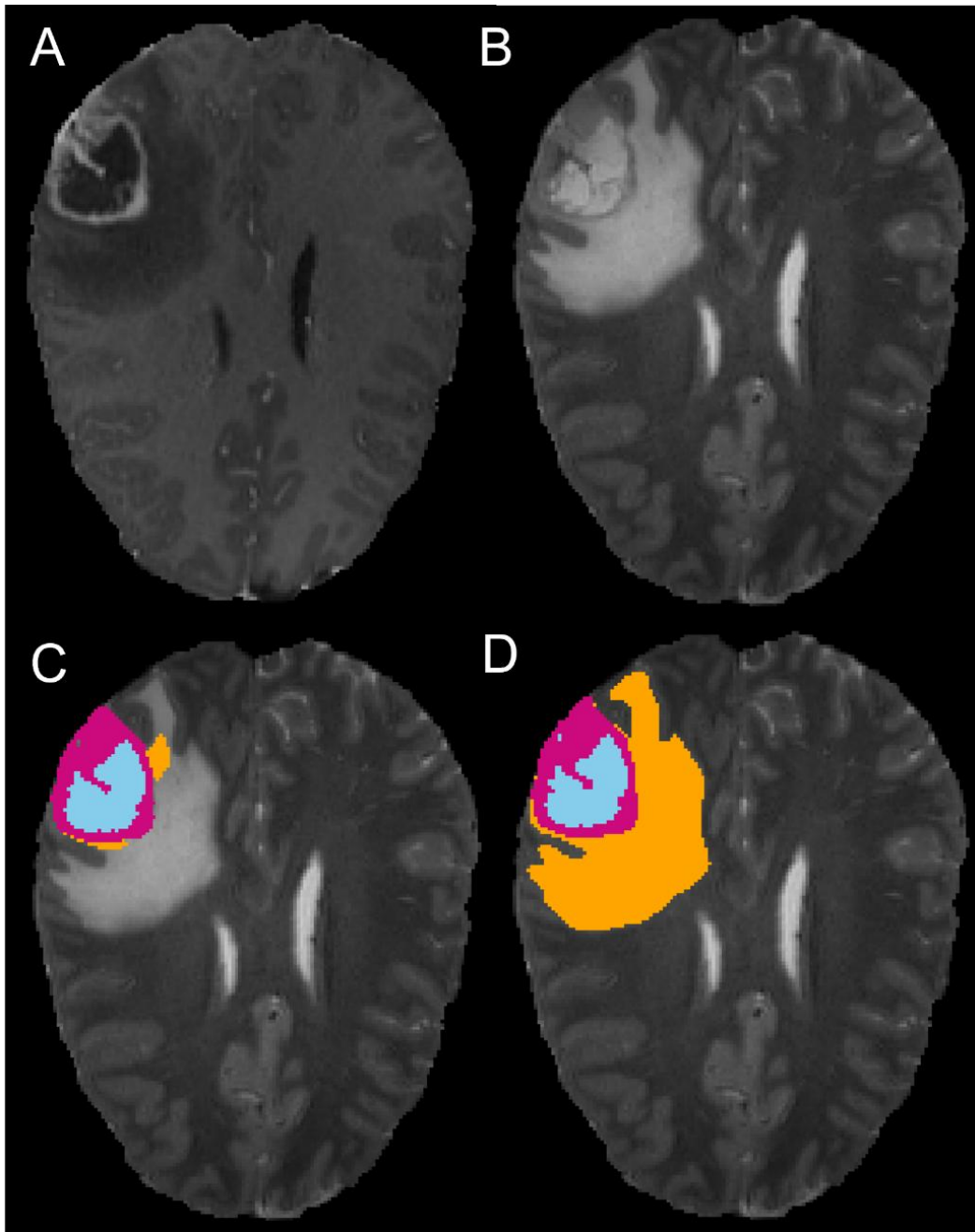


Figure 1: Representative external test case (UPenn-GBM). Qualitative comparison of predictions in the T2-FLAIR-absent inference scenario (T2-FLAIR channel replaced with zeros). (A) T1 post-contrast and (B) T2-FLAIR for reference standard. (C) output of the region-wise nnU-Net trained without dropout ($r=0.0$) and T2-FLAIR absent and (D) output of the region-wise nnU-Net trained with targeted T2-FLAIR dropout ($r=0.35$) and T2-FLAIR absent, illustrating the failure mode of whole-tumor under-segmentation without dropout and recovery with dropout.

Abbreviations: FLAIR = fluid-attenuated inversion recovery; r = dropout probability rate.

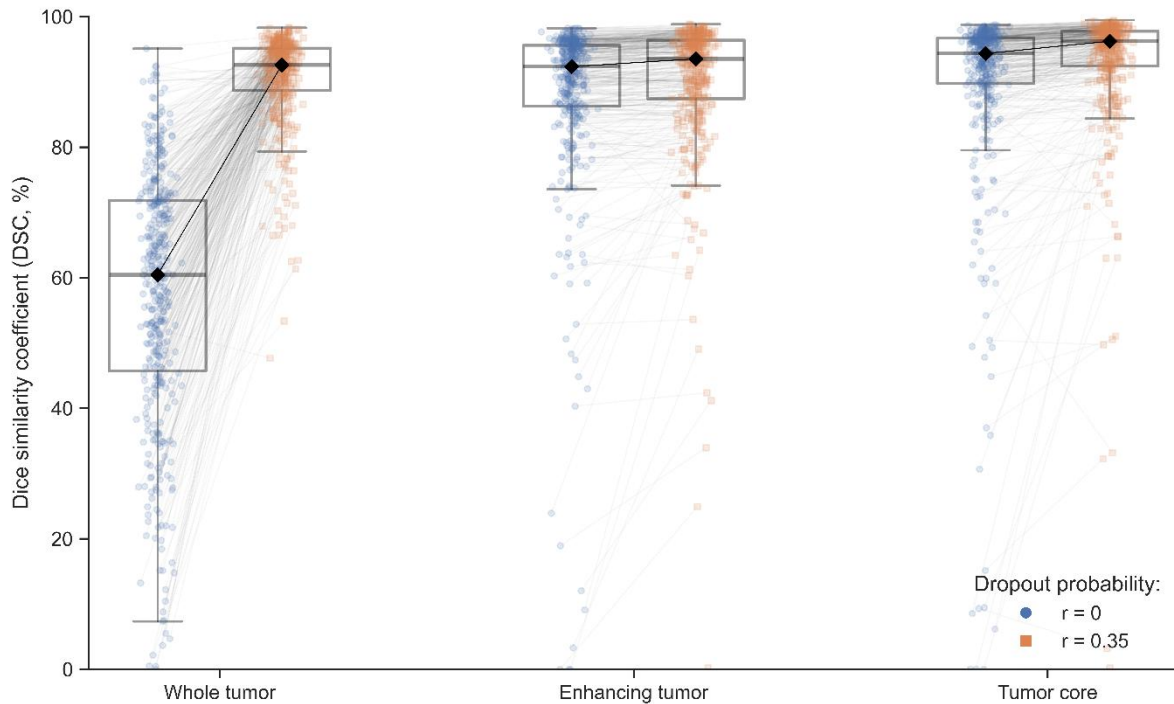


Figure 2: External testing on UPenn-GBM (n=403): region-wise model performance without T2-FLAIR. Per-patient Dice similarity coefficients (DSC, reported as %) for the region-wise models in the T2-FLAIR-absent inference scenario, comparing no-dropout training ($r=0.0$) versus targeted T2-FLAIR dropout training ($r=0.35$).

Abbreviations: DSC = Dice similarity coefficient; FLAIR = fluid-attenuated inversion recovery; r = dropout probability rate.

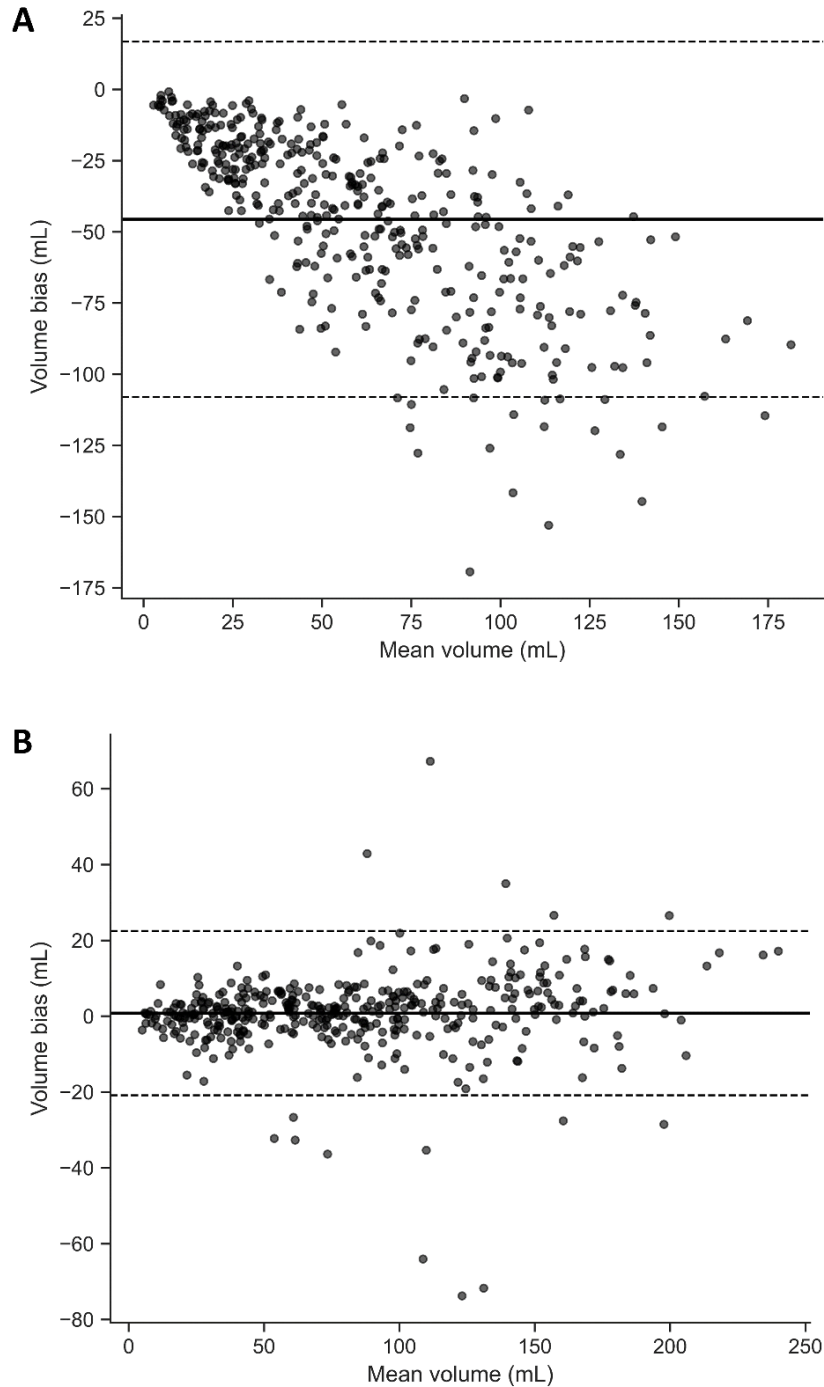


Figure 3: External testing on UPenn-GBM (n=403): Bland-Altman analysis of whole-tumor volume without T2-FLAIR. Bland-Altman plots of predicted minus reference standard whole-tumor volume (mL) in the T2-FLAIR-absent scenario for the region-wise nnU-Net trained (A) without dropout ($r=0.0$; Bias: -45.59 mL; Limits of Agreement: -107.96, 16.78 mL) and (B) with targeted T2-FLAIR dropout ($r=0.35$; Bias: 0.83 mL, Limits of Agreement: -20.83, 22.49 mL). Solid lines indicate mean bias; dashed lines indicate 95% limits of agreement. Abbreviations: FLAIR = fluid-attenuated inversion recovery; r = dropout probability rate.

Supplemental Materials

Supplementary Table S1: External testing on UPenn-GBM (n=403): segmentation performance of label-wise models with and without FLAIR at inference. Performance of label-wise nnU-Net models (NCR/NET, ED, ET) trained on BraTS 2021 with targeted T2-FLAIR dropout probability $r=0.0, 0.35, 0.50$ and evaluated under two prespecified inference scenarios: T2-FLAIR-present and T2-FLAIR-absent (T2-FLAIR channel replaced with zeros). Values are median [Q1-Q3] across patients. Overall denotes the unweighted macro-average across NCR/NET, ED, and ET.

Metrics/abbreviations: DSC = Dice similarity coefficient (reported as %); HD95 = 95th-percentile Hausdorff distance (mm); NCR/NET = necrotic and non-enhancing tumor; ED = edema; ET = enhancing tumor; FLAIR = fluid-attenuated inversion recovery; r = dropout probability rate.

	Overall		Enhancing Tumor		Non-enhancing Tumor		Edema	
T2-FLAIR drop for training	DSC med [Q1-Q3]	HD95 med [Q1-Q3]	DSC med [Q1-Q3]	HD95 med [Q1-Q3]	DSC med [Q1-Q3]	HD95 med [Q1-Q3]	DSC med [Q1-Q3]	HD95 med [Q1-Q3]
<i>Segmentation with T2-FLAIR input</i>								
$r=0.0$	91.0 [82.0-95.0]	2.01 [1.07-3.46]	94.0 [88.0-97.0]	1.00 [1.00-1.41]	91.0 [79.0-97.0]	1.41 [1.00-4.12]	92.0 [85.0-96.0]	1.73 [1.00-3.46]
$r=0.35$	91.0 [81.0-95.0]	2.00 [1.14-3.42]	94.0 [87.0-97.0]	1.00 [1.00-1.41]	92.0 [79.0-97.0]	1.41 [1.00-4.12]	92.0 [85.0-96.0]	1.41 [1.00-3.61]
$r=0.5$	90.0 [81.0-95.0]	2.04 [1.14-3.58]	94.0 [87.0-97.0]	1.00 [1.00-1.41]	91.0 [79.0-97.0]	1.41 [1.00-4.24]	91.0 [85.0-95.0]	1.72 [1.00-3.61]
<i>Segmentation without T2-FLAIR input</i>								
$r=0.0$	64.0 [55.0-71.0]	9.17 [6.53-13.06]	91.0 [84.0-95.0]	1.41 [1.00-2.24]	89.0 [72.0-96.0]	2.24 [1.00-5.20]	14.0 [3.0-28.0]	22.44 [16.43-31.03]
$r=0.35$	89.0 [79.0-93.0]	2.26 [1.41-4.06]	94.0 [87.0-96.0]	1.00 [1.00-1.41]	92.0 [79.0-97.0]	1.73 [1.00-4.24]	87.0 [78.0-92.0]	2.45 [1.73-4.69]
$r=0.5$	89.0 [79.0-94.0]	2.30 [1.38-4.17]	93.0 [87.0-96.0]	1.00 [1.00-1.41]	92.0 [76.0-97.0]	1.73 [1.00-4.36]	88.0 [79.0-92.0]	2.24 [1.73-4.64]

Supplementary Table S2: Supplementary Table S2. External testing on UPenn-GBM (n=403): equivalence testing (TOST) for $r=0.35$ vs $r=0.0$ across inference scenarios (label-wise). Paired comparison of label-wise models trained with targeted T2-FLAIR dropout ($r=0.35$) versus no dropout ($r=0.0$) under T2-FLAIR-present and T2-FLAIR-absent inference scenarios. Entries report the median paired DSC difference ($r=0.35 - r=0.0$) in DSC percentage points, with 95% bootstrap confidence intervals. TOST p-values test equivalence within ± 1.5 DSC percentage points ($\alpha=0.05$).

Abbreviations: TOST = two one-sided tests; DSC = Dice similarity coefficient; NCR/NET = necrotic and non-enhancing tumor; ED = edema; ET = enhancing tumor; r = dropout probability rate.

	Median DSC $r(0.35)-r(0)$ [95%CI]	TOST p-Value
<i>Segmentation with T2-FLAIR input</i>		
Overall	0.0442 [0.002, 0.092]	<0.001
ET	-0.0071 [-0.056, 0.027]	<0.001
NET	0.0320 [0.011, 0.074]	<0.001
Edema	-0.0417 [-0.078, 0.029]	<0.001
<i>Segmentation without T2-FLAIR input</i>		
Overall	24.1974 [23.613, 24.685]	1
ET	1.075 [0.916, 1.241]	1
NET	0.9508 [0.705, 1.213]	1
Edema	69.3675 [67.202, 70.926]	1

Supplementary Table S3: External testing on UPenn-GBM (n=403): equivalence testing (TOST) for $r=0.35$ vs $r=0.50$ across inference scenarios (label-wise). Paired comparison of label-wise models trained with targeted T2-FLAIR dropout probabilities $r=0.35$ versus $r=0.50$, evaluated under T2-FLAIR-present and T2-FLAIR-absent inference scenarios. Entries report the median paired DSC difference ($r=0.35 - r=0.50$) in DSC percentage points, with 95% bootstrap confidence intervals. TOST p-values test equivalence within ± 1.5 DSC percentage points ($\alpha=0.05$).

Abbreviations: TOST = two one-sided tests; DSC = Dice similarity coefficient; NCR/NET = necrotic and non-enhancing tumor; ED = edema; ET = enhancing tumor; r = dropout probability rate.

	Median DSC $r(0.35)-r(0.50)$ [95%CI]	TOST p-Value
<i>Segmentation with T2-FLAIR input</i>		
Overall	0.247 [0.183, 0.316]	<0.001
ET	0.188 [0.118, 0.233]	<0.001
NET	0.256 [0.171, 0.329]	<0.001
Edema	0.172 [0.122, 0.218]	<0.001
<i>Segmentation without T2-FLAIR input</i>		
Overall	-0.051 [-0.138, 0.013]	<0.001
ET	-0.007 [-0.067, 0.041]	<0.001
NET	0.0484 [0.000, 0.136]	<0.001
Edema	-0.234 [-0.301, -0.172]	<0.001

Supplementary File: CLAIM Checklist (2024 Update)

CLAIM item	Checklist requirement (paraphrased)	Addressed	Manuscript location	Notes
1	Identify the work as an AI/ML study in the title/abstract.	Yes	Title; Abstract header and text	
2	Provide a structured abstract that summarizes design, data, model, evaluation, and main results.	Yes	Abstract (Purpose/Materials and Methods/Results/Conclusion)	
3	Describe clinical/scientific background and intended use/role of the AI tool.	Yes	Introduction	
4	State study objective(s) and/or hypothesis(es).	Yes	End of Introduction (Purpose and hypotheses)	
5	Specify whether the study is prospective or retrospective.	Yes	Methods – Study design and reporting	
6	State study goal (e.g., model development, validation, noninferiority/equivalence, etc.).	Yes	Introduction, Methods	
7	Describe data sources (origin, dataset name(s), public/private, recruitment).	Yes	Methods – Datasets and reference standard (BraTS 2021; UPenn-GBM)	
8	Define inclusion/exclusion criteria and study setting/time frame.	Yes	Methods – Datasets and reference standard	
9	Describe preprocessing steps applied to the data.	Yes	Methods – Datasets and reference standard	BraTS organizer preprocessing is described
10	Describe any selection of subsets/regions/patches/frames for model input.	Yes	Methods – Training and testing	Extraction of UPenn GBM dataset for external validation dataset is described
11	Describe de-identification and privacy protection approach.	Yes	Methods – Study design and reporting	Only public de-identified datasets are used
12	Describe missing data and how it was handled.	NA	Methods	Full public dataset was used, which only contains subjects with full four modality imaging set
13	Provide imaging acquisition protocol details (scanner, sequences, key parameters) or cite where available.	Partial	Methods	BraTS is a heterogenous imaging dataset, parameters for each site are publicly available and referenced
14	Identify and justify the reference standard used.	Yes	Methods	
15	Describe how reference annotations/labels were generated.	Yes	Methods	
16	Define what constitutes a positive case / target definition(s).	Yes	Methods	Tumor subcompartments and derived regions are defined
17	Describe reference standard quality assurance (expertise, blinding, adjudication).	Yes	Methods	

CLAIM item	Checklist requirement (paraphrased)	Addressed	Manuscript location	Notes
18	Report inter- and/or intra-rater variability (and/or mitigation) for the reference standard.	NA		Ground truth segmentations obtained from BraTS dataset
19	Describe data partitioning for training/validation/testing (and sizes).	Yes	Methods	
20	State the level of disjointness between partitions (e.g., patient-level).	NA		
21	Describe how sample size was determined (power/precision or rationale).	Partial	Methods	No formal sample size calculation was performed, as all available data were used
22	Describe model architecture; cite prior architecture if used; describe modifications.	Yes	Methods	nnU-Net 3D full-resolution used, with region- and label-based training, with and without FLAIR-dropout at fixed proportions
23	Report software/frameworks and versions; provide access information when applicable.	Yes	Methods	
24	Describe model parameter initialization (including randomness/seed control).			
25	Describe training procedure and hyperparameters (optimizer, LR, epochs, augmentation, loss, early stopping).	Partial	Methods	Epochs and use of nnU-Net defaults are stated; consider adding a concise hyperparameter summary or nnU-Net plan/config file in Supplementary Methods.
26	Describe how the final model/checkpoint was selected.	Yes	Methods	
27	Describe any ensembling and how outputs were combined.	Yes	Methods	
28	Specify evaluation metrics and rationale/clinical relevance.	Yes	Methods – Statistics	
29	Describe statistical analysis and uncertainty estimation.	Yes	Methods – Statistics	
30	Describe robustness/sensitivity analyses.	Yes	Methods - Statistics	
31	Describe model explainability/interpretability methods (if used).	NA		
32	Report performance on internal data (training/validation/test as applicable).	NA		
33	Report performance on external data (if applicable).	Yes	Results; Supplementary	
34	Provide clinical trial registration information (if applicable).	NA		Retrospective analysis of public de-identified datasets; no

CLAIM item	Checklist requirement (paraphrased)	Addressed	Manuscript location	Notes
				registration expected.
35	Provide participant/data flow (numbers included/excluded) per cohort.	Yes	Methods	
36	Report participant demographics/clinical characteristics (when available).	Partial	Methods	BraTS demographics are briefly described and cited
37	Report performance metrics with measures of uncertainty (CI, IQR) and appropriate aggregation.	Yes	Results and Supplementary	Medians/IQRs and bootstrap CIs for paired differences are provided.
38	Report subgroup analyses (if performed) and pre-specification.	NA		
39	Provide analysis of errors/failures (qualitative or quantitative).	Yes	Results/Discussion	
40	Report interpretability outputs/results (if interpretability methods used).	NA		
41	Discuss limitations, biases, and generalizability.	Yes	Discussion – Limitations paragraph	
42	Discuss clinical implications and future work.	Yes	Discussion; Conclusion	
43	State availability of data, code, and/or trained model (or restrictions).	No	Data availability statement	
44	Report funding sources and role of funders.	Yes	Funding statement	.